Structural analysis of the indium-stabilized GaAs(001)-$c(8\times2)$ surface

T.-L. Lee*
Department of Materials Science and Materials Research Center, Northwestern University, Evanston, Illinois 60208 and European Synchrotron Radiation Facility, BP 220, F-38043 Grenoble Cedex, France

C. Kumpf
Experimentelle Physik II, Universität Würzburg, D-97074 Würzburg, Germany

A. Kazimirov and P. F. Lyman
Department of Materials Science, Northwestern University, Evanston, Illinois 60208

G. Scherb
Max-Planck-Institut für Festkörperforschung, Heisenbergstrasse 1, D-70569 Stuttgart, Germany

M. J. Bedzyk
Department of Materials Science and Materials Research Center, Northwestern University, Evanston, Illinois 60208 and Materials Science Division, Argonne National Laboratory, Argonne, Illinois 60439

M. Nielsen and R. Feidenhans'l
Condensed Matter Physics and Chemistry Department, Risø National Laboratory, DK-4000 Roskilde, Denmark

R. L. Johnson
II. Institut für Experimentalphysik, Universität Hamburg, D-22761 Hamburg, Germany

B. O. Fimland
Norwegian University of Science and Technology, N-7491 Trondheim, Norway

J. Zegenhagen
European Synchrotron Radiation Facility, BP 220, F-38043 Grenoble Cedex, France

(Received 05 February 2002; revised manuscript received 05 September 2002; published 4 December 2002)

The indium-stabilized GaAs(001)-$c(8\times2)$ surface was investigated by surface x-ray diffraction and x-ray standing waves. We find that the reconstruction closely resembles the $c(8\times2)$ structure described by the recently proposed unified model for clean III-V semiconductor surfaces [Kumpf *et al.*, Phys. Rev. Lett. **86**, 3586 (2001)]. Consistent with this unified model, no In dimers are found for the present surface. Instead, for coverages less than 0.25 monolayers, the In adatoms adsorb at the initially unoccupied hollow sites to form In rows along the [110] direction. Between the In rows, surface and subsurface Ga dimers are found to coexist in the trench areas. Above 0.25 monolayers, the additional In adatoms fill the trenches and replace the surface Ga atoms. The final structure of the surface layer is essentially identical to the InAs clean surface, except that the In heights are substantially different due to the lateral strain induced by the lattice mismatch. This structural difference explains why the ladder-type pattern observed previously by scanning tunneling microscopy only appears for the In/GaAs(001) and InAs/GaAs(001) surfaces, but not for the InAs clean surface. The structural model we propose for the In-stabilized GaAs(001)-$c(8\times2)$ surface, which fully agrees with the scanning tunneling microscopy results, should therefore generally apply to strained InAs(001) surfaces.

DOI: 10.1103/PhysRevB.66.235301 PACS number(s): 68.35.Bs, 68.43.Fg, 61.10.Eq, 68.49.Uv

I. INTRODUCTION

Due to a large lattice mismatch, InAs/GaAs has served as an ideal system for studying the thermodynamics for the epitaxial growth of highly strained heterostructures. It is well established that two-dimensional (2D) growth of InAs on GaAs(001) can only occur during the nucleation of the first two monolayers (ML's).[1] Recent investigations have shown that the planar growth is immediately followed by the formation of self-organized, coherent three-dimensional (3D) InAs islands,[2] which has opened up an opportunity for realization of novel devices utilizing the 3D quantum-confinement effect.[3] For applications where 2D growth is more desirable, it was found that under an In-rich condition the growth of 3D islands becomes completely inhibited and the formation of misfit dislocations can be significantly delayed.[4–7]

Despite this interesting behavior and potential technological applications, a complete understanding of the atomic-scale structures at the initial growth stage of InAs on the GaAs(001) is still absent. This is particularly true for the surface reconstructions induced by the In-rich growth condition. Resch-Esser *et al.*[8] reported the first scanning tunneling microscopy (STM) study of the In-terminated GaAs(001) $(4\times2)/c(8\times2)$ surface prepared by depositing a sub-ML of In on the GaAs(001) (2×4) surface, followed by an anneal at 450–480 °C. For an In coverage $\Theta_{In}=0.25$ ML their

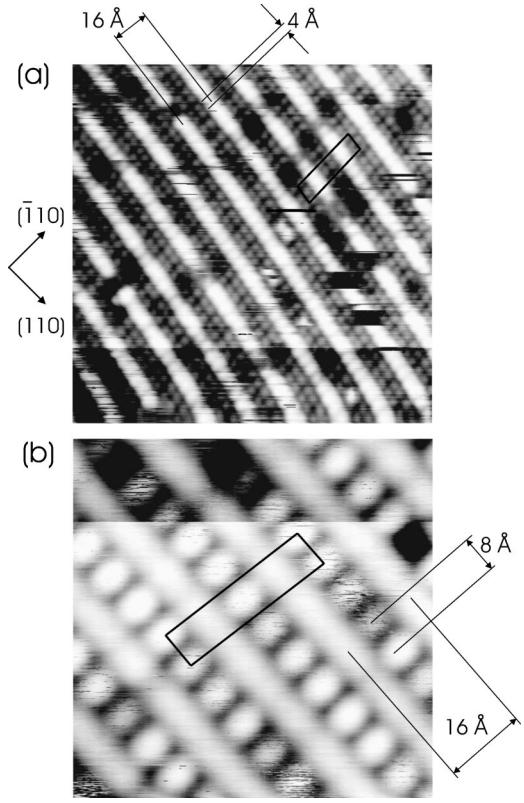

FIG. 1. High-resolution STM images of In-terminated GaAs(001)-$c(8\times2)$ surface reported by Resch-Esser *et al.* in Ref. 8 with $\Theta_{In}=$ (a) 1/4 and (b) 1/2 ML. The $c(8\times2)$ unit cells are marked by the rectangles.

filled-state image [reproduced in Fig. 1(a) for convenience] revealed straight rows parallel to the [110] direction separated by 16 Å, leading to the $4\times$ period. The bright ovals that made up the straight rows appeared to have a 4-Å periodicity along the rows. In addition, four faint corrugation maxima per 4×2 unit cell in a 1×1 symmetry were clearly resolved in the trench areas between the straight rows. As the Θ_{In} increased, additional protrusions, spaced by 8 Å along the [110] direction, gradually filled the trenches until a ladder-type pattern was completely formed at $\Theta_{In}=0.5$ ML [Fig. 1(b)]. Similar features were later observed by Xue *et al.*[7] in a STM investigation for 0.6 ML of In on GaAs(001). Most interestingly, Behrend *et al.*[9] and Belk *et al.*[10] showed that the STM images measured from the $c(8\times2)$ surfaces of 10–20 ML's of strained InAs grown under an In-rich condition on GaAs(001) were also characterized by this ladder-type pattern.

Figures 2(a) and (b) depict the structural models for the $(4\times2)/c(8\times2)$ surface proposed by Resch-Esser *et al.*[8] and Xue *et al.*,[7] respectively. Despite containing two In dimers per 4×2 unit cell in the topmost layer for both models, Resch-Esser *et al.* attributed the straight rows observed in the STM images to In dimers, while Xue *et al.* assigned them to As dangling bonds in the second layer. In addition to this striking difference, the agreement between the model and the STM data is in neither case satisfactory. Furthermore, these two models were mostly constructed on the basis of our earlier understanding of the structure for the Ga-rich GaAs(001) clean surface,[11] which was derived by analogy from the better-known As-rich counterpart. New evidence from theoretical calculations and low-energy electron diffraction (LEED),[12] as well as surface x-ray diffraction (SXRD),[13,14] has very recently shown that the $c(8\times2)$ structures of the group-III-rich III-V clean surfaces feature subsurface group-III dimers and are far more complex than the previously accepted models. It is therefore necessary to re-evaluate the existing $c(8\times2)$ models for the In/GaAs(001) surface.

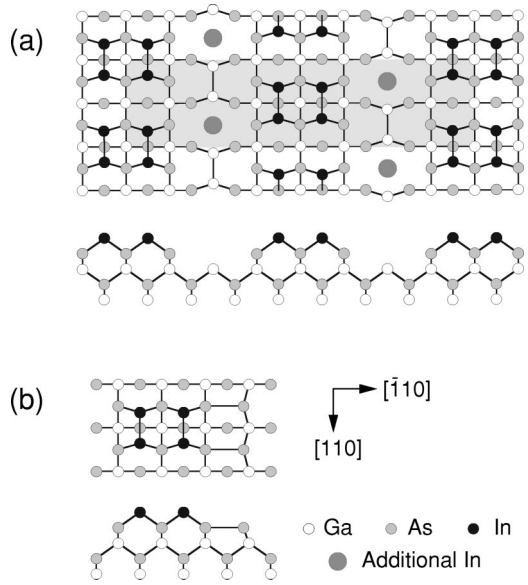

FIG. 2. Structural models proposed previously by (a) Resch-Esser *et al.* (Ref. 8) and (b) Xue *et al.* (Ref. 7) for the GaAs-$(4\times2)/c(8\times2)$-In surface.

In the present work we investigate the $c(8\times2)$ structure of the In-stabilized GaAs(001) surface with SXRD and x-ray standing waves (XSW) using synchrotron radiation. It will be shown that the final structure of the surface layer is essentially identical to the InAs clean surface reported in Ref. 13, except that the In heights are substantially different due to the lateral strain induced by the lattice mismatch. The $c(8\times2)$ model concluded from the present study shows general agreement with the previous STM observations.

II. EXPERIMENT

The GaAs(001) substrates were prepared prior to the x-ray measurements with a 1-μm-thick homoepitaxial layer by molecular-beam epitaxy. Thus prepared smooth surfaces were then protected by an amorphous As layer for sample transfer in air. The SXRD experiment was carried out at the BW2 wiggler beamline of the Hamburger Synchrotronstrahlungslabor (HASYLAB), and XSW experiments were conducted at beamline X15A of the National Synchrotron Light Source (NSLS) at Brookhaven National Laboratory and 12ID-D at the Advanced Photon Source. For each preparation, after introduction into the MBE system at the beamline, the GaAs substrate was first degassed at 250 °C for about one hour. The As protective layer was then removed by ther-

mal desorption at 350 °C. The As-rich $(2\times4)/c(2\times8)$ reconstructed surface was attained by annealing the sample further at 400–450 °C. Indium was deposited from a Knudsen cell held at 730 °C with the substrate held at room temperature (RT), followed by a 20-min anneal at 470 °C.[8] The LEED pattern thereafter exhibited a $(4\times2)/c(8\times2)$ symmetry. The surface prepared for the SXRD measurement was further characterized by STM to ensure a good surface quality and the desired In coverage of 1/4 ML. For the XSW measurement the In coverage was estimated to be approximately $0.3(\pm0.1)$ ML, based on comparison of the In MNN to As LMM peak-height ratio with the ratio measured from a sample calibrated by Rutherford backscattering.

For the SXRD experiment, the sample was transferred *in situ* to a small mobile ultrahigh vacuum (UHV) chamber, which was later mounted on a *z*-axis diffractometer. An in-plane data set was measured at $E\gamma=8.0$ keV. The integrated intensity of each reflection was measured by rotating the sample about its surface normal (ω scans). The peaks were then integrated, background subtracted, and corrected in the standard manner for Lorentz factor, polarization factor, active sample area, and rod intercept.[15] Since the (001) surface of the zinc-blende structure has only twofold rotational symmetry, there is only one domain rotationally. By averaging equivalent reflections using the $c2mm$ symmetry of the $c(8\times2)$ supercell a systematic error in $|F|^2$ of $\epsilon=7.4\%$ was determined, indicating the good quality of the data set. The final data set consists of 64 nonequivalent in-plane reflections. Similar to the situation reported for the InAs clean surface in Ref. 14 no eighth-order reflections could be measured. Therefore the data set consists of the (4×1) subcell reflections only. Standard LEED coordinates ($\mathbf{a}=1/2[1\bar{1}0]_{\text{bulk}}$, $\mathbf{b}=1/2[110]_{\text{bulk}}$, $\mathbf{c}=1/4[001]_{\text{bulk}}$) are used in the following discussion.

For the XSW experiment the prepared sample was transferred *in situ* to a connected x-ray chamber. Each XSW measurement involved scanning the incident x-ray energy (equivalent to scanning the angle of the sample) through a particular GaAs *hkl* Bragg reflection.[16] During these eV-wide scans, the phase of the standing wave shifts by 180° with respect to the *hkl* diffraction planes. With an incident photon energy E_γ above the In *L* edges ($E_{L_2}=3.938$ keV and $E_{L_3}=3.730$ keV), the induced modulation of the In *L* fluorescence yield, which depends strongly on the locations of the In atoms, was monitored by a solid-state Si(Li) detector. To triangulate the In positions we employed the GaAs(004) reflection at $E_\gamma=7.3$ keV, along with the (022), $(\bar{1}11)$, and (111) reflections at $E_\gamma=6.2$ keV.

III. DATA ANALYSIS AND RESULTS

A. SXRD

The analysis of two-dimensional Patterson functions is often used as a first step in determining surface structures. This reveals interatomic distances within the unit cell and in many cases a starting model can be derived for further least-square refinement. The Patterson function is calculated from the measured intensities $|F_{hk0}|^2$ of the in-plane reflections $(hk0)$ using the equation

$$P(x,y)\propto\sum_{h,k}|F_{hk0}|^2\cos[2\pi(hx+ky)]. \tag{1}$$

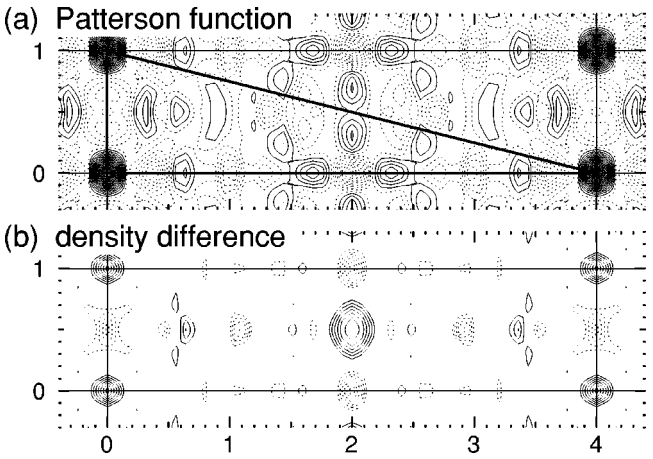

FIG. 3. Contour maps of (a) the experimental Patterson function and (b) the density difference. (a) was evaluated from the measured in-plane data set for the GaAs-$c(8\times2)$-In surface. (b) is the difference between the electron densities of the model for the clean surface (see Ref. 14) and those calculated from the measured structure factors for the In-covered surface neglecting differences in the phases of the structure factors.

Figure 3(a) shows the contour plot of the measured Patterson function for the surface under study. Positive peaks in the map correspond to interatomic distance vectors within the unit cell projected onto the surface plane. It is instructive then to compare this map directly with the one published recently for the GaAs(001)-$c(8\times2)$ clean surface [see Fig. 2(a) in Ref. 14]. The overall agreement between them is striking and thus suggests that the In-covered GaAs surface adopts basically the same structure as the clean surface. Nevertheless, the structural modification due to In adsorption can be realized if one compares the 2D-electron densities deduced from the model and measured structure factors. We calculate the density difference using

$$\begin{aligned}\triangle\rho(x,y,0)&=\rho_{expt}(x,y,0)-\rho_{model}(x,y,0)\\&\propto\sum_{h,k}\{(|F_{hk0,expt}|-|F_{hk0,model}|)\\&\quad\times\cos[2\pi(hx+ky)-\varphi_{hk0}]\},\end{aligned}$$

where φ_{hk0} is the phase for the calculated structure factor $F_{hk0}=|F_{hk0}|\exp(i\varphi_{hk0})$. The phase differences between the calculated and measured structure factors are neglected, since they are not accessible in a diffraction experiment. A contour plot of the density difference between the measured data for the In-covered GaAs(001)-$c(8\times2)$ surface and model for the clean surface taken from Ref. 14 is shown in Fig. 3(b). The only significant peaks appear at coordinates (0,0) and (2,0.5), indicating that the model lacks electron

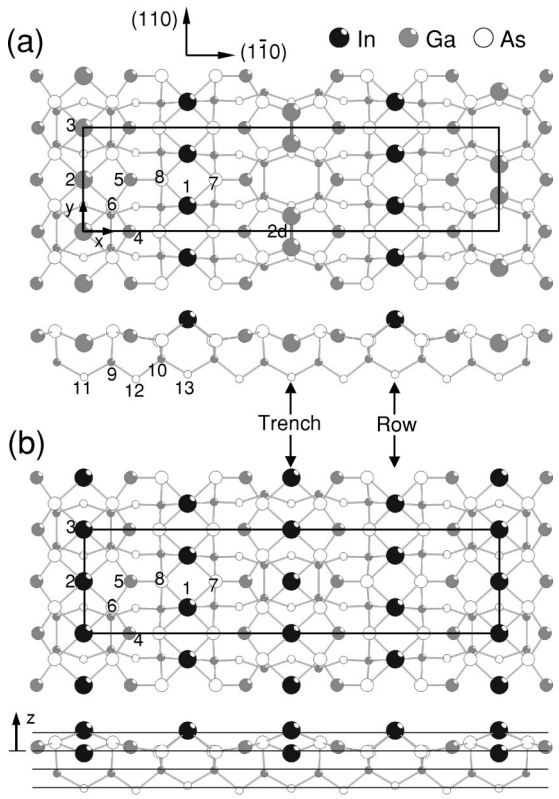

FIG. 4. Top and side views of the structural models for the GaAs-$c(8\times2)$-In surface deduced from the present (a) SXRD (model I, $\Theta_{In}\leqslant0.25$ ML) and (b) XSW (model II, $\Theta_{In}>0.25$ ML) analysis. In constructing the side views, the Ga and As atoms are tentatively placed vertically at the *z* coordinates for the GaAs clean surface in Ref. 14. The $c(8\times2)$ unit cell is indicated by the rectangular boxes. The main atoms in the structure are numbered. Below 0.25 ML, the In adatoms occupy only site 1 and form rows along the [110] direction. The trenches are populated with Ga monomers (sites 2 and 3) and Ga dimers (site 2*d*). Above 0.25 ML, the Ga atoms in the trenches are replaced by the additional In at sites 2 and 3. The horizontal lines in the side view of (b) denote the GaAs(004) planes extrapolated from the substrate lattice. Bonds are shown to assist viewing rather than to denote the ''true'' chemical bonds.

density at the sites 1, 2, and 3 in Ref. 14. This also suggests that the In adatoms fill mostly those sites which were not fully occupied on the Ga-rich GaAs(001)-$c(8\times2)$ clean surface.

For the refinement of the surface structure, no out-of-plane atomic positions could be evaluated since the data set consisted of in-plane data only. The *z* coordinates were therefore fixed to the values found previously for the GaAs clean surface.[14] This also applied to all the coordinates of the atoms in the deeper layers ($z\leqslant-0.75$ Å). Therefore only 14 positional parameters had to be refined, together with a varying number of occupancies and Debye-Waller (DW) factors as described below. The 14 refined atomic sites are labeled and denoted in Fig. 4, following the same convention used in Refs. 13 and 14.

In the first series of tests the surface Ga atoms located at sites 1–5 were replaced—one by one—by indium. Only the

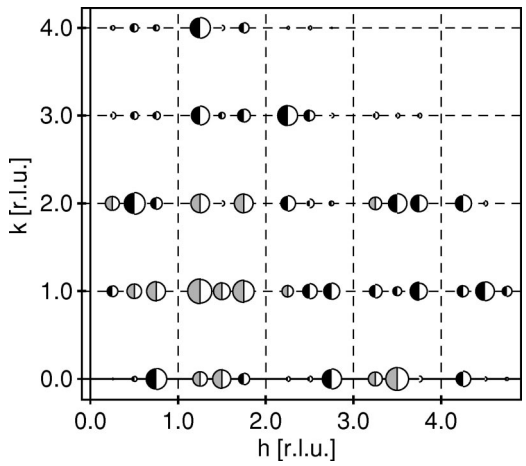

FIG. 5. In-plane data set for the In/GaAs-$c(8\times2)$ surface. *h* and *k* are given in units of the GaAs(001)-(1×1) surface unit cell based on the standard LEED coordinates (see text). The areas of the filled and open semicircles represent measured and calculated intensities, respectively. The gray/white circles have been scaled by a factor of 0.5 with respect to the scale of the black/white circles.

positional parameters and the occupancies of the Ga/In sites were refined, and no DW factors were considered. None of these fits resulted in a χ^2 below 8.0 except the model with indium at site 1, yielding $\chi^2=7.2$. Since the reduction in χ^2 was not significant, further tests were performed with two and three Ga sites being occupied simultaneously by In. This did not lead to a noticeable improvement in the fit ($\chi^2\geqslant7.0$), and thus the possibility for In occupying more than one site was rejected.[17]

In the next step, the DW factors were allowed to vary in addition to the set of parameters from the first series of tests. The only fit showing a significant reduction of χ^2 (to 4.8) was achieved by placing indium at site 1 with a high DW factor of 12.2. Introducing anisotropic DW factors for the In at site 1 reduced the χ^2 value further to $\leqslant1.5$. In the *x* and *z* directions this fit rendered DW factors reasonably close to the bulk values, whereas in the *y* direction a much larger DW factor was reached, indicating disorder to some extent along the [110].[18] Since occupancies and DW factors are often highly correlated, decreasing the number of these parameters was necessary to improve the stability of the fit. This was achieved by introducing constraints for the Ga occupancies for sites 2, 2*d*, and 3 and by using only one unique DW factor for all uppermost Ga atoms (sites 2–5). A common DW factor for the As sites 7 and 8 could be found as well. The indium atom at site 1 was described by two anisotropic DW factors, and only $DW_x(=DW_z)$ was refined. In the final fit ($\chi^2=1.57$) 19 parameters (14 positional, two occupancies, and three DW factors) were allowed to vary. Compared to 64 independent measurements this number of free parameters is reasonably small. The corresponding model (model I) and the in-plane data set are depicted in Figs. 4(a) and 5, respectively, and all parameters are listed in Table I.

B. XSW

Figures 6(a)–(d) show the results of the four XSW measurements. Based on dynamical diffraction theory, the fluo-

TABLE I. Atomic parameters for the GaAs-$c(8\times2)$-In surface determined by SXRD for $\Theta_{In}\leq 0.25$ ML (model I). The positions are compared with the coordinates for the GaAs-$c(8\times2)$ clean surface (Ref. 14) (column 3). All the in-plane positions are given in LEED coordinates, z coordinates in unit of GaAs d_{004}, deviations in Å, and Debye Waller (DW) factors in Å^2. All the listed z coordinates are fixed to the values for the GaAs clean surface and all the DW factors are isotropic, except those for the In atoms (see text). DW factors not listed in the table were fixed at their bulk values: $DW(\mathrm{Ga})=1.43$ Å^2 and $DW(\mathrm{As})=0.87$ Å^2. The given standard deviations were calculated assuming uncorrelated parameters. Values listed without error were not refined due to the $c2mm$ symmetry constraints.

Site	Position in In/GaAs	Position in GaAs	Deviation **d** (Å) [a]	$\lvert\mathbf{d}\rvert$ (Å)	DW(Å^2)	Occupancy
1 (In)	2.000, 0.500, 1.308	2.000,0.500,1.308 [b]	0.000,0.000	0.000	[c]	0.70(2)
2d (Ga)	4.000, 0.301(4), −0.100	4.000,0.293,−0.100	0.000,0.030	0.030	1.61(9)	0.59(2)
2 (Ga)	0.000, 1.000, [d]	not occupied			1.61(9)	0.41(2)
3 (Ga)	0.000, 0.000, [d]	not occupied			1.61(9)	0.41(2)
4 (Ga)	0.879(2),0.000, 0.316	0.870,0.000,0.316	0.040,0.000	0.040	1.61(9)	
5 (Ga)	0.907(2),1.000, 0.284	0.883,1.000,0.284	−0.095,0.000	0.095	1.61(9)	
6 (As)	0.556(1),0.500(5),0.556	0.540,0.511,0.556	−0.061,0.045	0.076	1.75(9)	
7 (As)	1.457(2),0.000, 0.036	1.461,0.000,0.036	−0.015,0.000	0.015	0.90(9)	
8 (As)	1.505(2),1.000, 0.060	1.474,1.000,0.060	−0.125,0.000	0.125	0.90(9)	
9 (Ga)	0.524(1),0.319(2),−1.152	0.526,0.330,−1.152	0.011,0.043	0.044		
10 (Ga)	1.488(1),0.470(3),−0.976	1.484,0.530,−0.976	−0.012,0.238	0.238		
11 (As)	0.000, 0.500(4),−1.968	0.000,0.492,−1.968	0.000,−0.031	0.031		
12 (As)	1.004(1),0.483(3),−2.076	1.013,0.498,−2.076	0.039,0.061	0.073		
13 (As)	2.000, 0.500, −1.920	2.000,0.500,−1.920	0.000,0.000	0.000		

[a]Since no z movement is allowed for all atoms only the (x,y) deviations are listed.
[b]For the clean GaAs surface this is a Ga site with an occupancy of 19%.
[c]This site shows anisotropic DW factors: $DW_x=DW_z=3.4(4)$ Å^2 and $DW_y=25$ Å^2 (not refined).
[d]The z coordinates of site 2 and 3 are fixed to the z coordinate of site $2d$ for the GaAs clean surface in the present analysis.

rescence yield from an adsorbate can be described as a function of the incident angle θ as[16]

$$Y(\theta)=Y_{\mathrm{OB}}\{1+R(\theta)+2\sqrt{R(\theta)}f_{\mathbf{H}}\cos[\nu(\theta)-2\pi P_{\mathbf{H}}]\}, \tag{2}$$

where $R(\theta)$ is the reflectivity, $\nu(\theta)$ is the phase of the standing wave, and Y_{OB} is the off-Bragg yield, i.e., the fluorescence yield for $R=0$. The coherent fraction ($f_{\mathbf{H}}$) and coherent position ($P_{\mathbf{H}}$) are the amplitude and phase, respectively, of the complex **H**th Fourier component ($G_{\mathbf{H}}$) for the spatial distribution of the adatoms, i.e., $G_{\mathbf{H}}=f_{\mathbf{H}}\exp(2\pi i P_{\mathbf{H}})$. Geometrically $f_{\mathbf{H}}$ and $P_{\mathbf{H}}$ measure the width and center, respectively, of the atomic distribution along the **H** direction.

We start our data analysis by determining the four Fourier components of the indium distribution using χ^2 fits of Eq. (2) to the XSW data. The best fits obtained by varying $f_{\mathbf{H}}$, $P_{\mathbf{H}}$, and Y_{OB} are plotted as black solid lines in Figs. 6(a)–(d) and the corresponding values of $f_{\mathbf{H}}$ and $P_{\mathbf{H}}$ are listed in Table II. In the subsequent analysis, a number of structural models are considered and refined by a least-squares minimization of

$$S=\sum_{\mathbf{H}}|G_{\mathbf{H},\mathrm{mod}}-G_{\mathbf{H},\mathrm{exp}}|^2, \tag{3}$$

where $G_{\mathbf{H},\mathrm{mod}}$ and $G_{\mathbf{H},\mathrm{exp}}$ are the model-calculated and XSW-measured Fourier components, respectively. To calculate $G_{\mathbf{H},\mathrm{mod}}$ we decompose $G_{\mathbf{H}}$ into a product of three factors based on the convolution theorem,

$$G_{\mathbf{H}}=CA_{\mathbf{H}}D_{\mathbf{H}}, \tag{4}$$

where C is the fraction of adatoms at ordered positions, and

$$A_{\mathbf{H}}=\sum_j g_j e^{2\pi i\mathbf{H}\cdot\mathbf{r}_j}, \tag{5}$$

is the geometrical structure factor that accounts for multiple occupation sites, where fractions Cg_j of the adatoms are located at $\mathbf{r}_j$. The expressions for geometrical factors of the models to be discussed below are listed in Table III for the four chosen Bragg reflections. In Eq. (4) $D_{\mathbf{H}}$ is related to the isotropic DW factor through $D_{\mathbf{H}}=\exp(-DW/2d_{\mathbf{H}}{}^2)$. Throughout the following analysis $DW=1.5$ Å^2, corresponding to a thermal vibrational amplitude $\sqrt{\langle u^2\rangle}=\sqrt{DW}/2\pi=0.195$ Å, is assumed for the In adsorbate.[19]

We consider first the in-plane structural model deduced from the SXRD study (model I). It is found that for $\Theta_{\mathrm{In}}\leq 1/4$ ML, the $c(8\times2)$ reconstruction is composed of a surface termination essentially the same way as the recently resolved GaAs(001)-$c(8\times2)$ structure by Kumpf *et al.*[13,14] with additionally all the In atoms occupying the hollow site (site 1 in Fig. 4) surrounded by four top-layer As atoms (sites 7 and 8 in Fig. 4). Given the in-plane position for site 1, the geometrical factor $A_{\mathbf{H}}$ can be derived in z_1 and C (Table III). The parameter z_1 is defined to be the In height, in unit of the GaAs (004) d spacing $d_{004}(=1.413$ Å), above the bulk extrapolated (004) plane that is best aligned with the As at sites 7 and 8 [see Fig. 4(b)]. By varying z_1 and C, the value of the least square S reaches its minimum at $S=0.167$. The corresponding values of z_1, C, $f_{\mathbf{H}}$, and $P_{\mathbf{H}}$ are tabulated in Table II and the resulting yield curves are plotted as center lines in

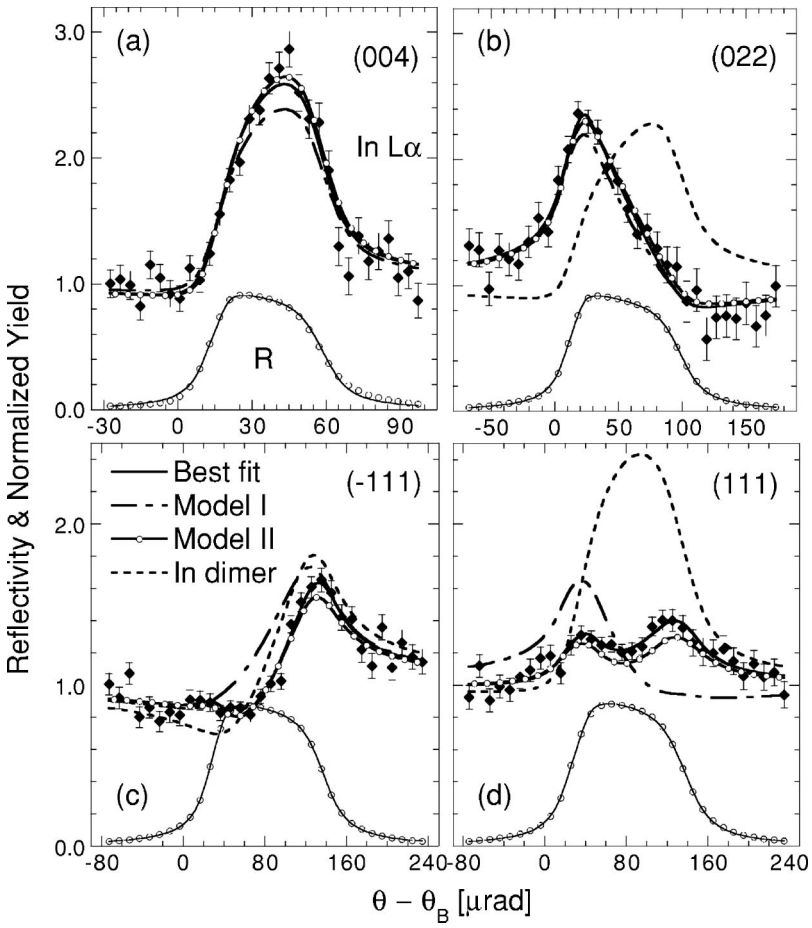

FIG. 6. Measured and calculated reflectivities R and normalized In $L\alpha$ fluorescence yields versus the incident angle θ for the GaAs (a) (004), (b) (022), (c) $(\bar{1}11)$, and (d) (111) XSW measurements for the GaAs-$c(8\times2)$-In surface. In the fluorescence analysis, the solid lines represent the best fits of Eq. (2) to the data. The center lines and solid lines with circles are the calculated In yields which minimize Eq. (3) for models I and II, respectively. The dashed lines simulate the In yields based on an In-dimer model (see text).

TABLE II. Measured and calculated Fourier components ($f_{\mathbf{H}}$ and $P_{\mathbf{H}}$) for the In atomic distribution of the $c(8\times2)$ surface for the GaAs(004), (022), $(\bar{1}11)$, and (111) reflections from the XSW analysis ($\Theta_{\mathrm{In}}>0.25$ ML). The calculations were based on models I and II and the In-dimer model. Also listed are the geometrical parameters (g_1, g_2, z_1, z_2, z_3, L, and C) and the least-square S obtained from the model analysis (see text).

	In dimer	Model I	Model II	Measured
g_1	1.0	1.0	0.484±0.02	
z_1	1.140	1.136	1.204±0.03	
g_2			0.304±0.02	
z_2			−0.044±0.06	
z_3			1.215±0.03	
L	0.720			
C	0.670	0.496	0.934±0.05	
f_{004}	0.460	0.341	0.490	0.46±0.04
P_{004}	0.140	0.136	0.146	0.14±0.02
f_{022}	0.354	0.411	0.395	0.43±0.03
P_{022}	0.070	0.568	0.534	0.54±0.02
$f_{\bar{1}11}$	0.624	0.462	0.571	0.59±0.02
$P_{\bar{1}11}$	0.035	0.034	0.985	0.99±0.02
f_{111}	0.398	0.462	0.395	0.37±0.02
P_{111}	0.035	0.534	0.650	0.66±0.02
S	1.143	0.167	0.0045	

Figs. 6(a)–(d) for the analysis based on model I. The reasonable agreement between the calculated coherent positions and their measured counterparts for the (004), (022), and $(\bar{1}11)$ reflections indicates that In monomers positioned at site 1 is indeed able to account for the main feature of the $c(8\times2)$ surface. However, it is also evident from the plots that modification to this model is needed to achieve a better agreement for the (111) reflection.

In the $c(8\times2)$ model proposed for the InAs clean surface by Kumpf *et al.*,[13,14] the unit cell contains additional, fourfold coordinated In sites in the trench areas between the In rows considered above. Two nonequivalent sites have been identified along these trenches: those As hollows between (site 2) and above (site 3) the subsurface In dimers [Fig. 4(b)]. The vertical position of site 3 was found to be 0.91 Å higher than site 2 due to the In dimers underneath. It is also worth noticing that the in-plane positions of sites 2 and 3 are 180° out of phase with respect to site 1 in the [110] direction. Since Θ_{In} was estimated to be slightly above 0.25 ML for the In-terminated GaAs surface under investigation here, it is reasonable to consider in our analysis sites 2 and 3 as additional In adsorption sites. Table III lists the expressions for the geometrical factors $A_{\mathbf{H}}$ for this model (model II), where z_2 and z_3 are defined similarly as z_1 (see Fig. 4), and Cg_1, Cg_2, and $C(1-g_1-g_2)$ are the fractions of the In adatoms occupying sites 1, 2, and 3. Minimizing the least square S by

TABLE III. Formulas for calculating the In geometrical structure factors $A_{\mathbf{H}}$ [Eq. (5)] for the GaAs(004), (022), $(\bar{1}11)$, and (111) reflections, based on models I and II and the In-dimer model.

	In dimer	Model I	Model II
A_{004}	$e^{2\pi i z_1}$	$e^{2\pi i z_1}$	$g_1 e^{2\pi i z_1}+g_2 e^{2\pi i z_2}+(1-g_1-g_2)e^{\pi i z_3}$
A_{022}	$-i\cos[\pi(1-L)]e^{\pi i z_1}$	$e^{\pi i z_1}$	$g_1 e^{\pi i z_1}+g_2 e^{\pi i(z_2+1)}+(1-g_1-g_2)e^{\pi i(z_3+1)}$
$A_{\bar{1}11}$	$e^{0.5\pi i z_1}$	$e^{0.5\pi i(z_1+3)}$	$g_1 e^{0.5\pi i(z_1+3)}+g_2 e^{0.5\pi i(z_2+3)}+(1-g_1-g_2)e^{0.5\pi i(z_3+3)}$
A_{111}	$-i\cos[\pi(1-L)]e^{0.5\pi i z_1}$	$e^{0.5\pi i(z_1+1)}$	$g_1 e^{0.5\pi i(z_1+1)}+g_2 e^{0.5\pi i(z_2+3)}+(1-g_1-g_2)e^{0.5\pi i(z_3+3)}$

varying g_1, z_1, g_2, z_2, z_3, and C leads to a significant reduction of S to 0.0045. The excellent agreement can also be seen clearly in Figs. 6(a)–(d), where the solid lines with circles, representing the calculated In yields for model II, nearly reproduce the best fits (the solid lines) for all four reflections. All the parameters and the calculated $f_{\mathbf{H}}$ and $P_{\mathbf{H}}$ are summarized in Table II.

For comparison we have also evaluated other structural models proposed previously for the In/GaAs(001)-$c(8\times2)$ reconstruction. One common feature of these models[8,7] is that they all consider In, Ga, or even As dimers as the building blocks for constructing the topmost layer of the $c(8\times2)$ unit cell. Despite the different detailed configurations among these models, all the In dimers are virtually equivalent with respect to the present XSW measurements. Therefore it is sufficient for the present XSW analysis to consider only one symmetric In dimer positioned at the modified bridge site. The bonding geometry of the In dimer can be described by the dimer height z_1 and the dimer bond length L (in unit of $a_{\mathrm{GaAs}}/\sqrt{2}=3.997$ Å). Minimizing S based on the $A_{\mathbf{H}}$ listed in Table III by allowing z_1, L, and C to vary results in a small S of 0.123 but an unphysical $L=0.294$ ($=1.175$ Å). Since reducing L from 1.0 to zero is equivalent to shifting the In atoms from the bridge site towards the hollow site, the result of this exercise has already suggested that the latter adsorption site is strongly favored. By fixing the In dimer bond length at twice the In covalent radii $2r_{\mathrm{In}}=2.88$ Å (or $L=0.720$) and adjusting only z_1 and C, the minimum of S increases drastically to 0.769 and only very low coherent fractions $f_{\mathbf{H}}$ are obtained. To make a more meaningful comparison we finally plot in Figs. 6(b)–(d) the simulated In yield curves as dashed lines using $z_1=1.14$ and $C=0.67$, based on the (004) XSW measurement, and $L=0.720$ (see Table II). For the (022) [Fig. 6(b)] and (111) [Fig. 6(d)] reflections, this In dimer model, which includes the possibility for subsurface dimerization of In, renders In yield curves completely out of phase with respect to the data and can be therefore safely ruled out.

IV. DISCUSSION

For $\Theta_{\mathrm{In}}\leqslant1/4$ ML on GaAs, the in-plane structure deduced from SXRD (model I) indicates that site 1 is strongly favored over sites 2 and 3 for the In adsorption, leading to the straight rows along the [110] direction observed in the STM images. The In atoms are separated by 16 Å between the rows and by 4 Å along the rows. The trench areas are terminated primarily with surface Ga dimers (site $2d$), as is the case for the GaAs $c(8\times2)$ clean surface,[13,14] except that additional occupation of Ga monomers at sites 2 and 3 were detected. The direct support for this model can be found in the STM images reported by Resch-Esser *et al.*[8] [Fig. 1(a)], where the As dangling bonds in the trenches are clearly resolved as four faint spots per 4×2 unit cell for $\Theta_{\mathrm{In}}\leqslant1/4$ ML, and they appear to be aligned in the $[1\bar{1}0]$ direction with the In atoms in the rows (site 1). Notice that the surface Ga atoms in the trenches are totally invisible to STM in this case. The SXRD results also show that the unique subsurface Ga dimer structure found for the clean surface remains upon the In adsorption, and is most responsible for the weak $\times2$ period observed in LEED.

Except for the In atoms positioned at site 1, the structure of this surface is virtually identical to the $c(8\times2)$ clean surface. This immediately explains why the In-stabilized $c(8\times2)$ reconstruction can also be formed at RT when the GaAs substrate exhibits the same symmetry prior to the In deposition, as observed recently by STM:[20] the highly mobile In adatoms can easily reach site 1 and become readily trapped in the hollows surrounded by the As dangling bonds. By contrast, extensive mass transport involving not only the In atoms but also the top few layers of GaAs are necessary for the transition from the (2×4) to the $c(8\times2)$, which can only occur at an elevated temperature. In the trench areas, the SXRD measurement shows that Ga surface dimers are the major structure for lower Θ_{In}, and the XSW analysis suggests that they should be eventually replaced by In for higher Θ_{In} upon annealing at 470 °C.

For $\Theta_{\mathrm{In}}>1/4$ ML on GaAs, the above XSW analysis based on model II concludes that for the present $c(8\times2)$ surface about 7% of the adsorbed In is random, 45% is located at site 1, 28% at site 2, and 20% at site 3. In Table IV we compare the XSW-determined In vertical positions with the relevant surface coordinates reported recently for the InSb, InAs, and GaAs $c(8\times2)$ clean surfaces by SXRD.[13,14] If we adopt the positions of the As at sites 7 and 8 determined for the GaAs clean surface measurement in Ref.[14], based on the present XSW result the In adsorbed at site 1 on GaAs is estimated to be 1.63 Å in average above the surrounding As atoms. This In height reduces to 1.51 Å for the InAs clean surface, i.e., the In becomes about 8% higher on GaAs. Since the local environment for the In at site 1 does not alter very much between these two terminations, the

TABLE IV. Comparison among the z coordinates of sites 1, 2, and 3 for the III-V $c(8\times2)$ clean surfaces (Ref. 14) and those determined from the present XSW study. Also listed are the z coordinates of the first-nearest-neighbor As/Sb (sites 6, 7, and 8) from Ref. 14. The average In-As distances $d_{\text{In-As}}$ for the In at sites 1, 2, and 3 are estimated for the In/GaAs(001) and InAs(001) clean surfaces based on the SXRD and XSW results.

	z (SXRD)			z (XSW)		$d_{\text{In-As}}$ (Å)
Site	InSb	InAs	GaAs	In/GaAs	InAs	In/GaAs
Row:						
1 (III)	0.798	1.018	(1.307)	1.204	3.38	3.37
7 (V)	0.120	0.049	0.035			
8 (V)	−0.018	−0.006	0.061			
Trench:						
2 (III)	−0.180	−0.004		−0.044	3.42	3.03
3 (III)	0.187	0.597		1.215	3.18	3.12
6 (V)	0.575	0.644	0.554			
a(Å)	6.479	6.058	5.653			

change of the In height reflects mostly the effect of epitaxial strain imposed by the substrates. The 7% reduction of the in-plane lattice parameters from InAs to GaAs leads to the lift of the In atoms at site 1 by the neighboring As while the average In-As distance remains essentially unchanged (Table IV).

For the In at site 2 the lateral strain shows a much smaller effect on its vertical position. However, a significant shortening of the In-As distance was estimated on GaAs (Table IV). This suggests a stronger interaction of the In with the underlying GaAs lattice at site 2, due to the shrinking of the void size. Most interestingly, the biaxial compression from the GaAs substrate has forced the In atoms at site 3 to protrude outward from the surrounding As at site 6, in clear contrast to the case for the InAs (InSb) clean surface, where the In stays below the As (Sb) level (Table IV). This shifting of the In's relative position from a concave to convex arrangement at site 3 is consistent with the different features observed by STM, where large periodic protrusions in the trenches have been clearly resolved for the In-terminated GaAs(001) surface[8,7,11] as well as the InAs/GaAs(001) surface,[9,10] whereas for the unstrained InAs and InSb surfaces the In atoms in the trenches have hardly been seen, even in the empty state images.[21–24] It is therefore evident that these pronounced protrusions in the STM images for the In/GaAs surface are In at site 3, and the ladder pattern made up of the protrusions uniquely marks the strained InAs surfaces. In addition, along the [110] direction between each pair of the adjacent protrusions there is most likely another In atom hidden at site 2, which cannot be detected by STM due to its much lower position. All together these In atoms exhibit a twofold periodicity along the trenches, following the same symmetry of the subsurface Ga dimers underneath. It is worth pointing out that in the high-resolution STM images reported by Xue *et al.*[7] the protrusions in the trenches and those in the rows are 180° out of phase in the [110] direction, supporting the model depicted in Fig. 4. Since the STM micrographs look remarkably similar for the In/GaAs(001) and InAs/GaAs(001) surfaces, the above In assignment should be generally applicable to the strained InAs $c(8\times2)$ surfaces.

Several authors[4–7,9,10] have demonstrated that by maintaining the $c(8\times2)$ reconstruction at the growth front the strain-driven 3D island formation of InAs on GaAs, which would normally occur at $\sim$1.5 ML's under an As-rich growth condition, can be completely suppressed. In addition to considering In as a virtual surfactant,[6] surface reconstruction may also play an important role in this morphological change. Among the newly developed $c(8\times2)$ models for the III-V surfaces,[12–14] one common feature is that all the outermost III-V layers tend to form a unique 2D network structure, which spans the trenches and interacts weakly with the underlying lattice. More theoretical studies are needed to verify whether this quasifloating layer functions as an effective structure for strain release at the surface.

V. SUMMARY

SXRD and XSW measurements were carried out to investigate the indium-stabilized GaAs(001)-$c(8\times2)$ surface. With the recent progress in solving the structures for the III-V semiconductor clean surfaces,[13,14] we conclude our present studies with a different structural model, which shows general agreement with the previous STM results. Contrary to the previously reported models, the $c(8\times2)$ reconstruction contains no In dimers. Instead, for coverages less than 0.25 monolayers, the In adatoms adsorb as monomers at the initially unoccupied hollow sites to form In rows along the [110] direction. Between the In rows, surface and subsurface Ga dimers are found to coexist in the trench areas, resembling the GaAs clean surface described in Ref. 13. The similarity between the In-terminated and clean $c(8\times2)$ structures makes it possible to form the former directly through an In deposition onto the latter at RT, as observed by STM.[20] Above 0.25 monolayers, the additional In adatoms fill the trenches and replace the surface Ga atoms. The final structure of the surface layer is essentially identical to the InAs clean surface,[13,14] except the In heights are substantially different due to the lateral strain induced by the lattice mismatch. This structural difference explains the unique ladder-type pattern observed in STM for the In/GaAs(001) and InAs/GaAs(001) surfaces. The structural model we propose should be therefore valid in general for strained InAs(001) surfaces.

ACKNOWLEDGMENTS

We would like to thank the HASYLAB staff for technical assistance. This work was supported by the U.S. Department of Energy Under Contracts No. W-31-109-ENG-38 to Argonne National Laboratory and No. DE-AC02-76CH00016 to the NSLS, by the National Science Foundation under Contracts No. DMR-9973436 to M.J.B. and No. DMR-0076097 to the MRC at Northwestern University, and by the Danish Research Council through Dansync and the IHP Program "Access to Research Infrastructures" of the European Commission (HPRI-CT-1999-00040).

*Corresponding author. Electronic address: tllee@esrf.fr

[1] D. Leonard, K. Pond, and P.M. Petroff, Phys. Rev. B **50**, 11 687 (1994); T.R. Ramachandran, R. Heitz, P. Chen, and A. Madhukar, Appl. Phys. Lett. **70**, 640 (1997).

[2] C.W. Snyder, B.G. Orr, D. Kessler, and L.M. Sander, Phys. Rev. Lett. **66**, 3032 (1991).

[3] For a review, see P.M. Petroff, A. Lorke, and A. Imamoglu, Phys. Today **54(5)**, 46 (2001).

[4] W.J. Schaffer, M.D. Lind, S.P. Kowalczyk, and R.W. Grant, J. Vac. Sci. Technol. B **1**, 688 (1983).

[5] H. Munekata, L.L. Chang, S.C. Woronick, and Y.H. Kao, J. Cryst. Growth **81**, 237 (1987).

[6] E. Tournie, O. Brandt, and K.H. Ploog, Appl. Phys. Lett. **60**, 2877 (1992); E. Tournie and K.H. Ploog, *ibid.* **62**, 858 (1993); E. Tournie, O. Brandt, K.H. Ploog, and M. Hohenstein, Appl. Phys. A: Solids Surf. **56**, 91 (1993); .E. Tournie, N. Grandjean, A. Trampert, J. Massies, and K.H. Ploog, J. Cryst. Growth **150**, 460 (1995); A. Trampert, E. Tournie, and K.H. Ploog, *ibid.* **146**, 368 (1995).

[7] Q. Xue, Y. Hasegawa, T. Ogino, H. Kiyama, and T. Sakurai, J. Vac. Sci. Technol. B **15**, 1270 (1997); Q. Xue, T. Ogino, H. Kiyama, Y. Hasegawa, and T. Sakurai, J. Cryst. Growth **175/176**, 174 (1997).

[8] U. Resch-Esser, N. Esser, C. Springer, J. Zegenhagen, W. Richter, M. Cardona, and B.O. Fimland, J. Vac. Sci. Technol. B **13**, 1672 (1995).

[9] J. Behrend, M. Wassermeier, and K.H. Ploog, J. Cryst. Growth **167**, 440 (1996).

[10] J.G. Belk, C.F. McConville, J.L. Sudijono, T.S. Jones, and B.A. Joyce, Surf. Sci. **387**, 213 (1997).

[11] For a review, see Q. Xue, T. Hashizume, and T. Sakurai, Prog. Surf. Sci. **56**, 1 (1997).

[12] S.-H. Lee, W. Moritz, and M. Scheffler, Phys. Rev. Lett. **85**, 3890 (2000).

[13] C. Kumpf, L.D. Marks, D. Ellis, D. Smilgies, E. Landemark, M. Nielsen, R. Feidenhans'l, J. Zegenhagen, O. Bunk, J.H. Zeysing, Y. Su, and R.L. Johnson, Phys. Rev. Lett. **86**, 3586 (2001).

[14] C. Kumpf, D. Smilgies, E. Landemark, M. Nielsen, R. Feidenhans'l, O. Bunk, J.H. Zeysing, Y. Su, R.L. Johnson, L. Cao, J. Zegenhagen, B.O. Fimland, L.D. Marks, and D. Ellis, Phys. Rev. B **64**, 075307 (2001).

[15] R. Feidenhans'l, Surf. Sci. Rep. **10**, 105 (1989); E. Vlieg, J. Appl. Crystallogr. **30**, 532 (1997).

[16] For a review on XSW method, see J. Zegenhagen, Surf. Sci. Rep. **18**, 199 (1993).

[17] This was also supported by the STM characterization on the same surface prior to the SXRD measurement, which showed topographical features very similar to those revealed in Fig. 1(a), indicating no In atoms in the trenches.

[18] This disorder along the [110] direction for the In adatoms at site 1 was also found for the InAs clean surface in the SXRD measurement in Ref. 14. However, it is not directly supported by the previous STM and present XSW studies. The large, anisotropic DW factors in the present SXRD analysis may result from the limited in-plane data set and missing of the eighth-order reflections.

[19] For all the models considered in the present XSW analysis, it was found that varying $DW(\mathrm{In})$ from 0.5 to 2.5 Å^2 caused only minor changes in the minimum of S and the final values of the geometrical parameters. This uncertainty of $DW(\mathrm{In})$ is included in the quoted error bars. It was also found that introducing anisotropic DW factors for the In did not improve the minimization any further.

[20] P. Vogt (private communication).

[21] S. Ohkouchi and N. Ikoma, Jpn. J. Appl. Phys., Part 2 **33**, L1770 (1994).

[22] C. Kendrick, G. LeLay, and A. Kahn, Phys. Rev. B **54**, 17 877 (1996).

[23] M.O. Schweitzer, F.M. Leibsle, T.S. Jones, C.F. McConville, and N.V. Richardson, Surf. Sci. **280**, 63 (1993).

[24] A.A. Davis, R.G. Jones, G. Falkenberg, L. Seehofer, R.L. Johnson, and C.F. McConville, Appl. Phys. Lett. **75**, 1938 (1999).